

Specific EXAFS Tools in Analysis of MoSI Nanowires[†]

Alojz Kodre^{1,2}, Jana Padežnik Gomilšek³, Iztok Arčon^{4,2}, Anton Meden⁵ and Dragan Mihailović^{1,2,6}

¹Faculty of Mathematics and Physics, University of Ljubljana, Jadranska 19, SI-1000 Ljubljana, Slovenia

²J. Stefan Institute, Jamova 39, SI-1000 Ljubljana, Slovenia

³Faculty of Mechanical Engineering, University of Maribor, Smetanova 17, SI-2000 Maribor, Slovenia

⁴Nova Gorica Polytechnic, Vipavska 13, SI-5000 Nova Gorica, Slovenia

⁵Faculty of Chemistry and Chemical Technology, University of Ljubljana, Aškerčeva 5, SI-1000 Ljubljana Slovenia

⁶Mo6 d.o.o. Teslova 30, SI-1000 Ljubljana, Slovenia

Received 23-05-2005

[†]Paper based on a presentation at the 14th International Symposium “Spectroscopy in Theory and Practice”, Nova Gorica, Slovenia, 2005.

Abstract

The structure of nanowires prepared by vapor synthesis from Mo, S and I is investigated by methods of x-ray diffraction (XRD) and extended x-ray absorption fine structure (EXAFS). Starting with a qualitative model of the structure from XRD, the metrics is introduced with interatomic distances determined from EXAFS. Two specific tools to increase the resolution of EXAFS method are discussed: the reciprocity relation between data from adjacent target atoms, and difference EXAFS from data on samples with small changes in stoichiometry.

Key words: EXAFS, nanowires, molybdenum sulphide-iodide.

Introduction

Vapor-synthesised sulfur-deficient Mo sulfides-iodides $\text{Mo}_6\text{S}_{9-x}\text{I}_x$ appear as woolly aggregates of long bundles of fine strands. In polar solvents, the strands can be separated as identical nanowires of ~ 8 Å diameter in the TEM scan. Judging from the separability, and from the high tensile strength and the low shear strength of the bundles, strongly bound polymer strands are held together in the bundle by weak Van der Waals forces. The material shows promise for a variety of nanotechnological applications.¹ To exploit its full potential, however, a detailed knowledge of its structure is instrumental. Following precision elemental analysis, the characterization of the structure is based on x-ray diagnostic techniques of XRD and EXAFS.

The XRD scan consists of an array of wide but well-defined diffraction peaks, from which the symmetry class of the material can be limited to a small family of related crystal groups with particular symmetry. An estimate for the size of the unit cell can also be obtained. However, the strong anisotropy of the material affects the XRD measurement so that the extracted symmetry class and parameters mainly relate to the lateral ordering

of the strands in the bundle while the dimension of the unit cell and the translational symmetry along the strand remain undefined.²

The study is an example of how the specific obstacles posed by the nanoscopic nature of the material can be overcome by a complementary application of the XRD and EXAFS techniques.

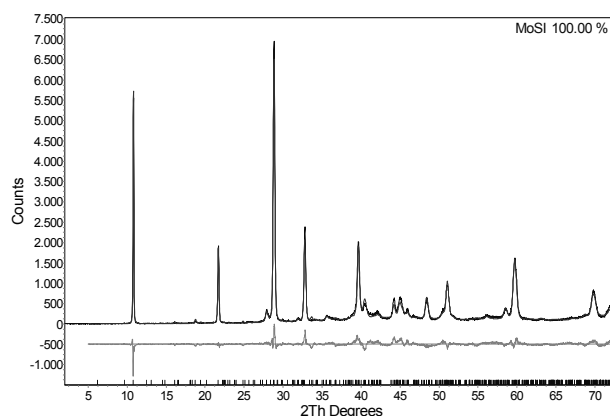


Figure 1. The XRD scan of the $\text{Mo}_6\text{S}_9\text{I}_6$ nanowire sample (x-axis – Bragg angle 2θ). The residue of the Rietveld fit is shown below (for details see reference 2).

Experimental

High quality Mo and I K edge EXAFS spectra for structural analysis of Mo sulfide-iodide $\text{Mo}_6\text{S}_{9-x}\text{I}_x$ samples with nominal stoichiometries $x = 6, 5,$ and 4.5 have been recorded in a standard transmission mode at the X1.1 beamline of HASYLAB at DESY (Hamburg, Germany), using a two-crystal Si 311 monochromator with an energy resolution of 3 eV at Mo K-edge (19.999 keV) and 6 eV at I K-edge (33.169 keV).³ The high-order harmonics were effectively eliminated by detuning of the monochromator crystals to the 60% of the rocking curve maximum, using the beam-stabilization feedback control. The intensities of the incident and transmitted beams were measured with three consecutive ionisation cells. For the Mo K-edge EXAFS the first cell was filled with 500 mbar Ar and 500 mbar N_2 , the second and the third were filled with 900 mbar Ar and 100 mbar Kr. For I K-edge EXAFS the first cell was filled with 900 mbar Ar and 100 mbar Kr, and the other two with 1000 mbar of Kr.

MoSI nanowire samples were homogeneously deposited on a filter paper. Several layers were stacked to obtain attenuation (μd) between 1.5 and 2 above the investigated K-edge. The absorption spectra were measured within the energy interval [-250 eV to 1000 eV] of the investigated K-edge. In the XANES region equidistant energy steps of 0.5 eV for Mo and 1.0 eV for iodine were used while for the EXAFS region equidistant k -steps ($\Delta k \approx 0.03 \text{ \AA}^{-1}$) were adopted with an integration time of 1s/step. The energy calibration of the monochromator was established with simultaneous absorption measurement on metallic Mo foil.

The spectra were analyzed by the UWXAFS program package using FEFF6 code for ab initio calculation of scattering paths.^{4,5}

Results and discussion

The XRD scan of the material, from which its hexagonal symmetry is deduced, is shown in Figure 1.

In EXAFS analysis of the neighborhood of a particular atom in the structure Fourier transforms of the signals are conventionally used for visualization since consecutive atomic neighbors of the investigated atom show up as consecutive peaks. Mo EXAFS spectra of the three samples (Figure 2) are remarkably similar showing combinations of the same constituents in slightly different proportions. Structural parameters are extracted from the spectra in the UWXAFS code by devising a model cluster of atoms and calculating the scattering pattern – an artificial EXAFS spectrum – from all possible scattering paths of the photoelectron in the cluster. By comparing the model spectrum to the measured one, and by relaxing the model parameters

towards the best fit of the two, the structure of the atomic neighborhood of the investigated atom is determined. A simple ansatz of the Mo atom neighborhood built of S, Mo and I atoms at contact distances (2.43 Å, 2.68 Å and 2.78 Å, respectively) explains completely the region of the Fourier transform below 3 Å. The respective coordination numbers of the neighbors, extracted from the scattering intensities are approximately 1.5, 4, and 2 per Mo atom. The four Mo neighbors are strongly indicative of an octahedron cluster: indeed, the fifth Mo neighbor at the distance $2.68\sqrt{2}$ Å is resolved with confidence from the spectrum upon expansion of the model by the corresponding scattering path.

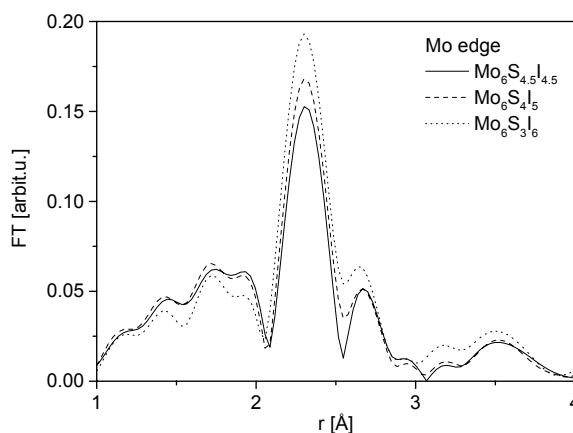


Figure 2. Fourier transforms of Mo K edge EXAFS spectra of three MoSI stoichiometries.

The I spectra of all three samples are identical within the noise level: the range below 3 Å contains only one prominent peak in the Fourier transform (Figure 3). The peak is explained by a shell of Mo neighbors at 2.83 Å. The relatively large width of the peak indicates a split shell. After the introduction of separate scattering paths, two close neighbor shells with normal widths, split by 0.1 Å are resolved.

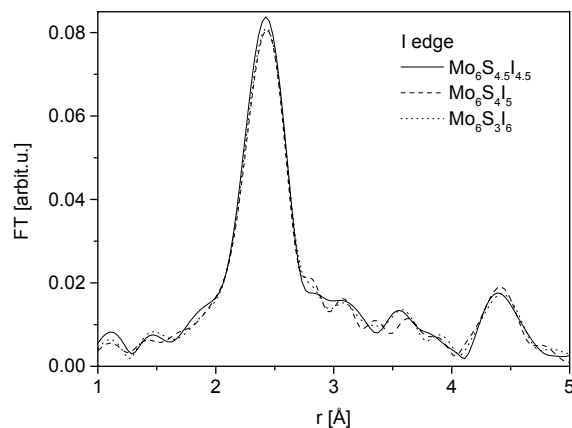


Figure 3. Fourier transforms of I K edge EXAFS spectra of three stoichiometries.

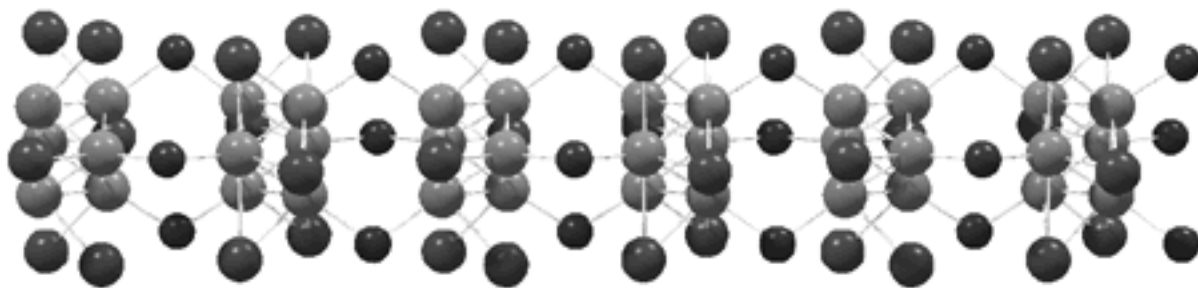


Figure 4. The proposed structure: six Mo octahedra (grey) of the polymer chain are shown, dressed and coupled with S (black-small) and I ions (black-large). The partition of the anions between the two sites may vary with stoichiometry.

A model of the structure of the strand - a chain of Mo octahedra coupled and dressed with S and I atoms - with the symmetry required by XRD (Figure 4) data has been devised on the basis of general valence and coordination considerations.² Metrics is introduced into the model by the inter-atom distances recovered from the EXAFS data.

The metric model is essential in improving the interpretation of the data in both methods. In XRD, the metric model offers a basis for a Rietveld refinement, with the satisfactory result shown in Figure 1. In EXAFS, the scattering paths of the UWXAFS code are read directly from the model structure, weeding out effectively the multitude of candidate paths of the contact cluster, growing ever denser with increasing inter-atom distance. In this way, a computationally feasible ansatz for the least-square fit of a wider neighborhood is constructed. Excellent fits, extending as far as 4.5 Å, are obtained with single-scattering paths from only 6 shells of neighbors (Figure 5). The contributions of all multiple-scattering paths are found negligible.

The structure parameters extracted from the Mo and I EXAFS signals are largely independent. The Mo-I scattering paths, however, contribute to both signals: the parameters of the paths, seen from either end, are linked with reciprocity relations.⁶ The values of the two geometric parameters of a path, namely the mean length and its dispersion, must be the same. The ratio of amplitudes of the path contribution in both signals equals to the inverse ratio of respective target atoms: in this way the number of bonds, counted from either end, is equal. In our spectra, the relations are fulfilled within the error bars of the parameters. The shortest Mo-I path is dominant in the I EXAFS and only the third in rank in Mo EXAFS, so that the accuracy of parameters extracted from the Mo signal is considerably lower. Even more: the narrow 0.1 Å splitting of the closest Mo-I distance distribution, well within the resolution of the I signal, remains unnoticed in the Mo signal.

Consequently, by fixing the Mo-I path parameters in the analysis of the Mo EXAFS at the values extracted from the I spectrum (including the splitting), the error intervals of the parameters of the neighbor shells beyond the first three contact neighbors are halved, so that the resolution of the analysis is markedly improved (Table I).

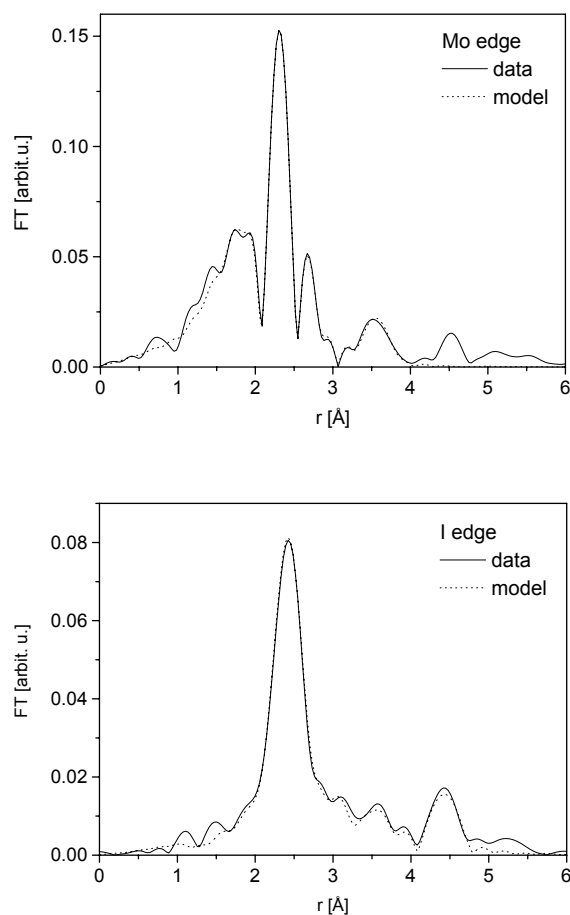


Figure 5. Comprehensive EXAFS model of Mo₆S₃I₆ for the Mo and I edge.

Table I. The first 6 neighbor shells of Mo and I in $\text{Mo}_6\text{S}_3\text{I}_6$, with reciprocity taken into account: atomic species, shell occupancy (N) and distance to the center atom (r) are given. The numbers in parentheses are standard deviations in the units of the last digit. The values without error are adopted from the model and not varied in the least-square procedure.

Mo neighborhood			I neighborhood		
atom	N	r [Å]	atom	N	r [Å]
S	1.45(9)	2.425	Mo	2	2.785(1)
Mo	4	2.675(2)	Mo	1	2.888(3)
I	2	2.785(4)	S	2	3.596(3)
I	1	2.890(4)	I	1	3.342(3)
Mo	1	3.774(3)	I	2	3.921(1)
S	2	4.376(4)	S	1	4.509(1)

The analysis of the Mo EXAFS of samples with different stoichiometries shows that only the S and I neighbor contributions vary while the Mo-Mo paths remain independent of the iodine content x , and consistent with the Mo octahedron as a basic building unit. To improve the resolution of the anion neighbors linking and girding the Mo octahedra, an idea of *difference EXAFS* seems promising: in the difference of two EXAFS signals, most easily performed in the wavevector space, the oscillatory components from neighbors, identically placed in both samples, should cancel out, leading to a signal with a simpler interpretation (Figure 6).

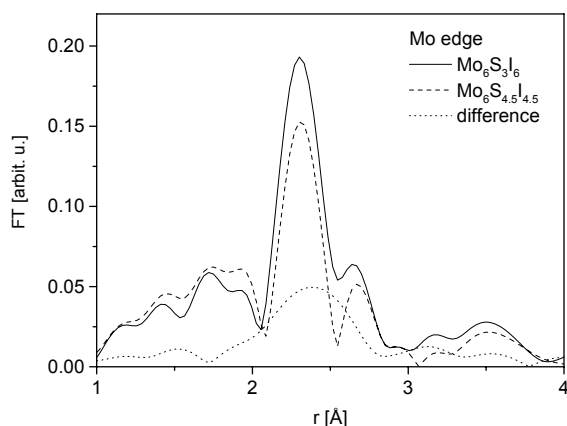


Figure 6. Fourier transforms of Mo EXAFS signals of samples with $x = 6$ and 4.5 and their difference EXAFS. Note that the subtraction is performed in the wavevector space and not in the complex space of the transforms, of which only the envelopes (absolute values) are shown.

In spite of the large noise level in the difference signal, the analysis yields definite results. The path parameters of the split I neighbor shell are fixed except for the amplitude which gives best-fit value of 0.24 neighbors, close to the stoichiometric value of 0.25 (change of 1.5 I atom neighbors for 6 Mo target atoms). The S neighbor shell appears, as expected, with

negative amplitude: however, beside the original contact distance of 2.43 Å, another small contribution at 2.77 Å is discerned, close to the radius of the shell of I atoms, which the S atoms substitute (Figure 7).

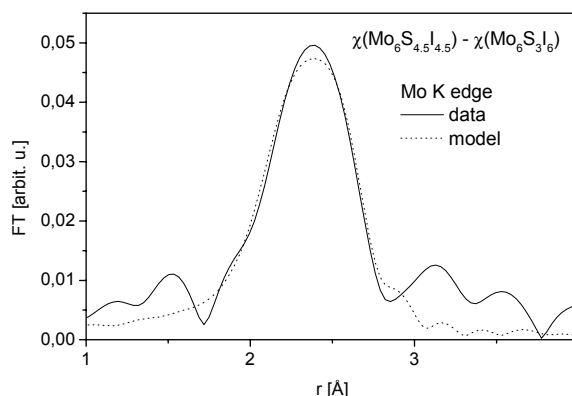


Figure 7. The difference EXAFS of the samples with maximum S and I content, and the model fit.

Conclusions

EXAFS structural analysis is instrumental in providing metrics to the models of structure based on XRD data. In the case of MoSI nanowires, the resolution of the EXAFS analysis is improved by two specific tools: (1) the reciprocity relations between parameters of common scattering paths in EXAFS signals of different target atoms, and (2) the difference EXAFS of samples with similar structure but different stoichiometries. The results are consistent with partial exchange of iodine and sulfur, with an assumption that the Mo core, together with the unexchanged I and S neighbors, remains completely unaffected. There is, however, an alternative explanation for the perfect cancellation of common components: the samples with three different x values contain the same compound, with varying amounts of an impurity – most likely a

Mo sulfide – introducing additional scattering paths and affecting the average atomic ratios.

Acknowledgements

This work was supported by the European Community - Research Infrastructure Action under the FP6 “Structuring the European Research Area” Programme (through the Integrated Infrastructure Initiative “Integrating Activity on Synchrotron and Free Electron Laser Science”). Support of Slovenian Ministry of Education, Science and Sport and the Internationales Buero of BMBF is acknowledged. We would like to thank Julia Wienold of HASYLAB station X1 for expert advice on beamline operation.

Povzetek

Z metodama rentgenske difrakcije (XRD) in podaljšane strukture rentgenskih absorpcijskih robov (EXAFS) smo raziskali strukturo nanožičk, dobljenih s sintezo par elementov Mo, S in I. V kvalitativni model strukture, postavljen na osnovi difrakcijske slike, uvedemo metriko s pomočjo medatomskih razdalj, ugotovljenih z metodo EXAFS. Podrobneje bomo obravnavali dve posebni orodji, s katerima izboljšamo ločljivost metode EXAFS: recipročne povezave, ki veljajo za prispevke sosednjih atomov v vzorcu, in diferenčni EXAFS za podatke iz vzorcev z majhnimi spremembami v stehiometriji.

References

1. M. Remškar, A. Mrzel, Z. Škraba, A. Jesih, M. Čeh, J. Demšar, P. Stadelman, F. Levy, D. Mihailović, *Science* **2001**, 292, 479–481.
2. A. Meden, A. Kodre, J. Padežnik Gomilšek, I. Arčon, I. Vilfan, D. Vrbanic, A. Mrzel, D. Mihailović, *Nanotechnology* **2005**, 16, 1578–1583.
3. A. Kodre, D. Vrbanic, J. Padežnik Gomilšek, I. Arčon, A. Mihelič, M. Hribar, *HASYLAB at DESY: Annual report 2004*, http://www-hasyllab.desy.de/science/annual_reports/2004_report/index.html
4. E. A. Stern, M. Newville, B. Ravel, Y. Yacoby and D. Haskel, *Physica B* **1995**, 208&209, 117.
5. J. J. Rehr, R. C. Albers and S. I. Zabinsky, *Phys. Rev. Lett.* **1992**, 69, 3397.
6. J. Batista, A. Pintar, J. Padežnik Gomilšek, A. Kodre, F. Bornette, *Appl. catal., A Gen.* **2001**, 217, 55–68.